Supporting information

Enhancing ORR Activity of Fullerene-Derived Carbons by Implanting Fe in Assembled Diamine-C_{60} Spheres

Bohong Jiang,[a#] *Suwei Wang,*[b#] *Fancang Meng,*[a] *Li Ju,*[a] *Wei Jiang,*[b]* *Qingmin Ji,*[a]* *Heng-Dao Quan* [c]

[1] Herbert Gleiter Institute for Nanoscience, School of Materials Science and Engineering, Nanjing University of Science & Technology, 200 Xiaolingwei, Nanjing, 210094, China

[2] National Special Superfine Powder Engineering Technology Research Center, Nanjing University of Science and Technology, 200 Xiaolingwei, Nanjing, 210094, China

[3] School of Chemistry and Chemical Engineering, Beijing Institute of Technology, 5 South Zhongguancun Street, Beijing 1000081, China

# These authors contributed this work equally

*Corresponding author: jiqingmin@njust.edu.cn, superfine_jw@126.com

Additional Data

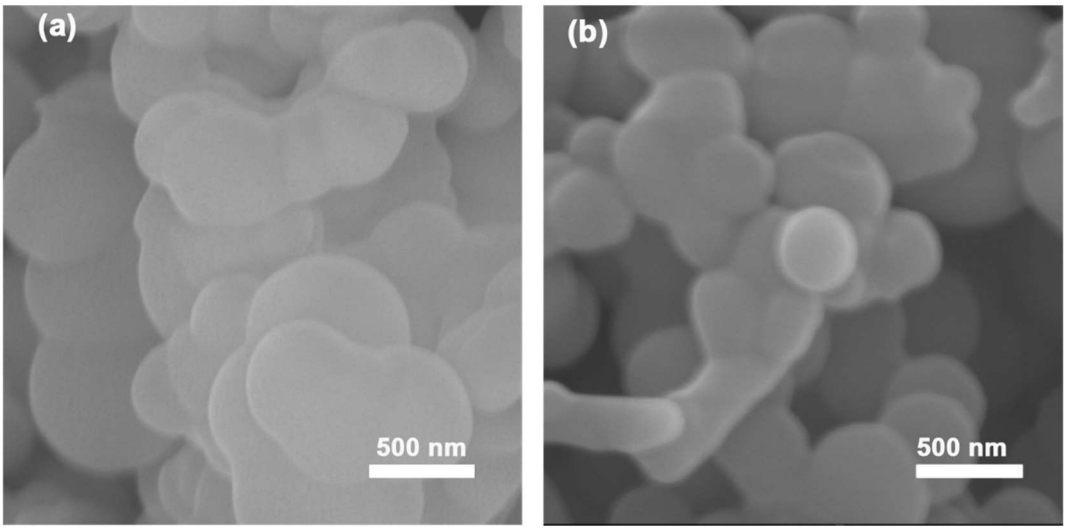

Fig. S1. SEM images of fullerene assembly structures at various mixing ratios of C_{60} and EDA, (a) C_{60}: EDA = 1:100, (b) C_{60}: EDA = 1:5000.

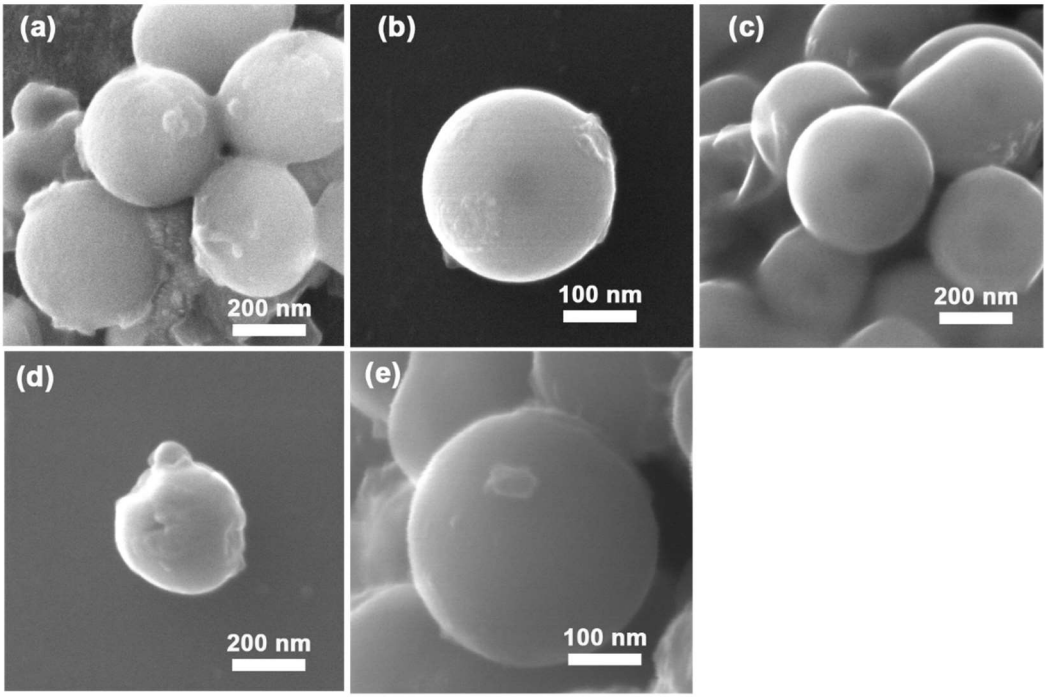

Fig. S2. SEM images of (a) N@FCS-500, (b) N@FCS-700, (c) N@FCS-900, (d) FeN@FCS-500 and (e) FeN@FCS-700.

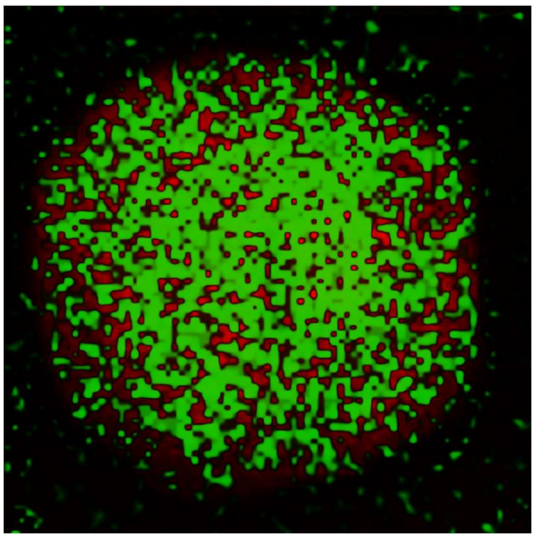

Fig. S3. The image of mixed elemental mappings of FeN@FCS-900 based on STEM observation and EDS analysis.

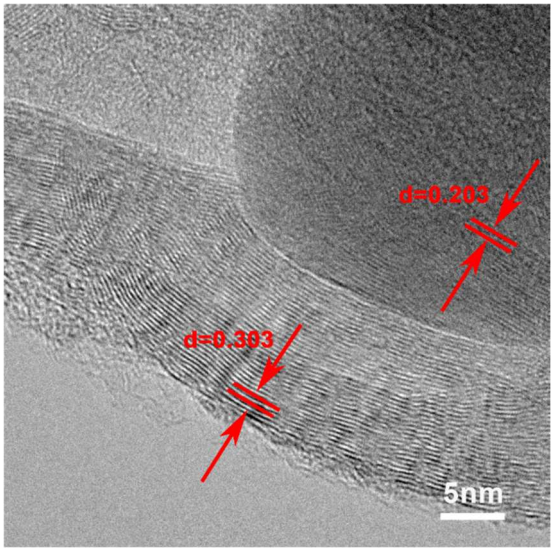

Fig. S4. HR-TEM image of FeN@FCS-900.

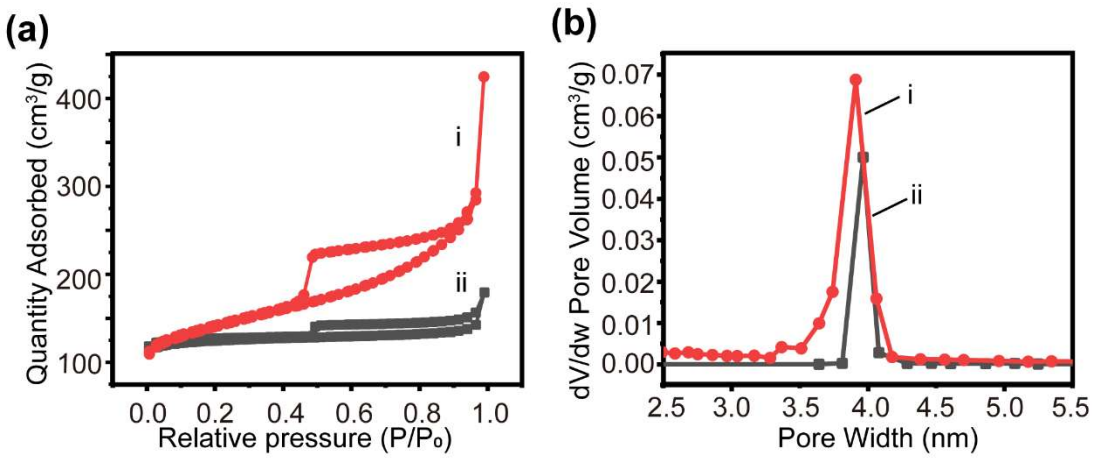

Fig. S5. (a) Nitrogen isotherms and (b) pore size distributions of (i) FeN@FCS-900 and (ii) N@FCS-900.

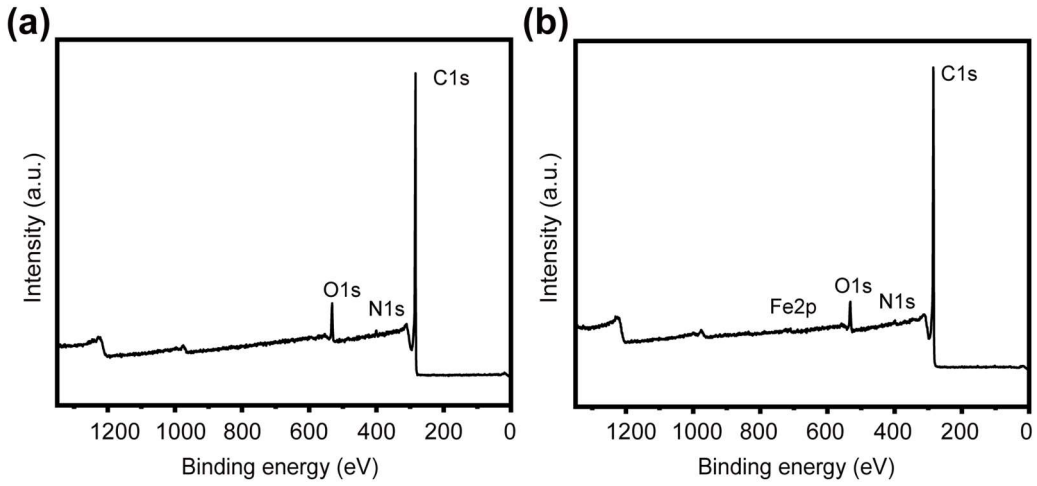

Fig. S6. Full-scan XPS spectra of (a) N@FCS-900 and (b) FeN@FCS-900.

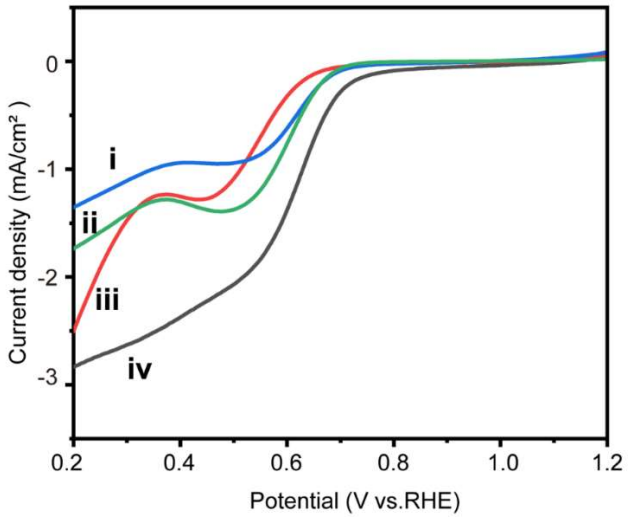

Fig. S7. LSV curves of (i) N@FCS-500, (ii) N@FCS-700, (iii) FeN@FCS-500 and (iv) FeN@FCS-700 in O_2-saturated 0.1 M KOH solution at 1600 rpm.

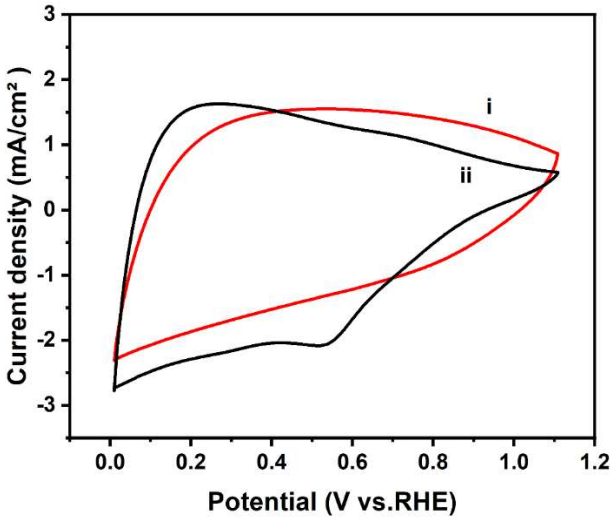

Fig. S8. CV curves of N@FCS-900 measured at scan rate of 10 $mV \cdot s^{-1}$ in (i) N_2-saturated 0.1M KOH solution, and (ii) O_2-saturated 0.1M KOH solution.

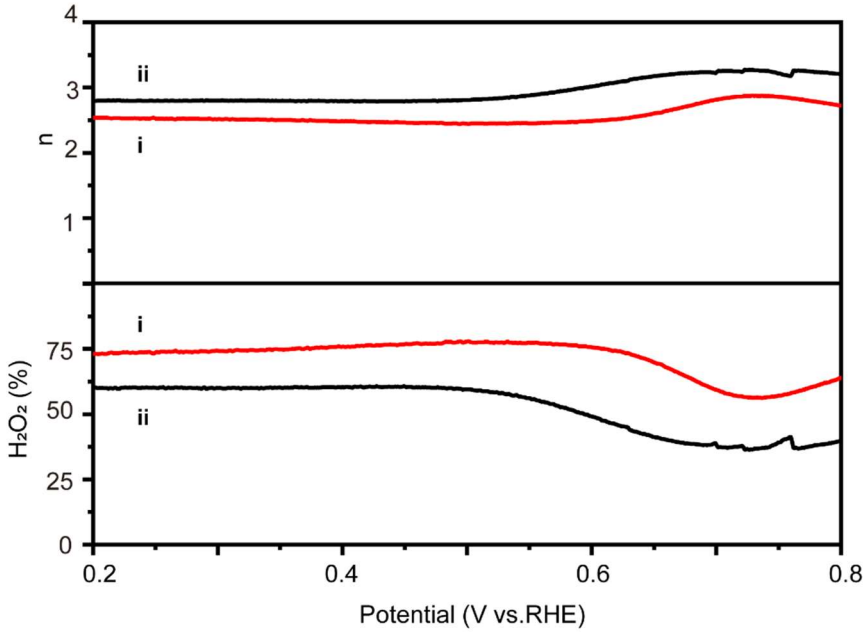

Fig. S9. The electron transfer number (n) and H_2O_2% yield of (i) C_{60}-900 and (ii) N@FCS-900.

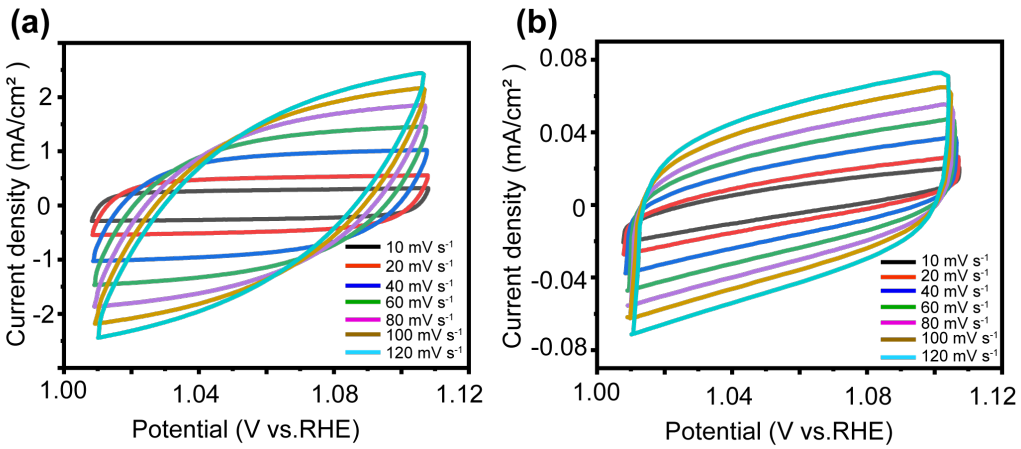

Fig. S10. CV curves of (a) FeN@FCS-900 and (b) N@FCS-900 measured in a non-Faradic region at different scan rates.

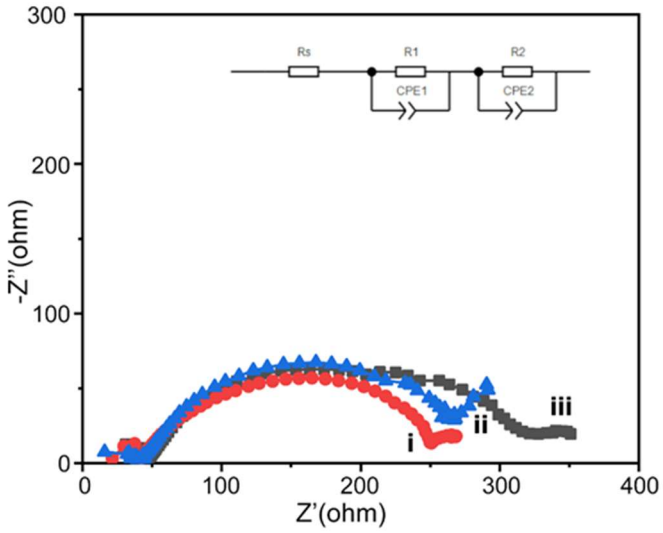

Fig. S11. Nyquist plots of (i) FeN@FCS-900, (ii) Pt/C, (iii) N@FCS-900.

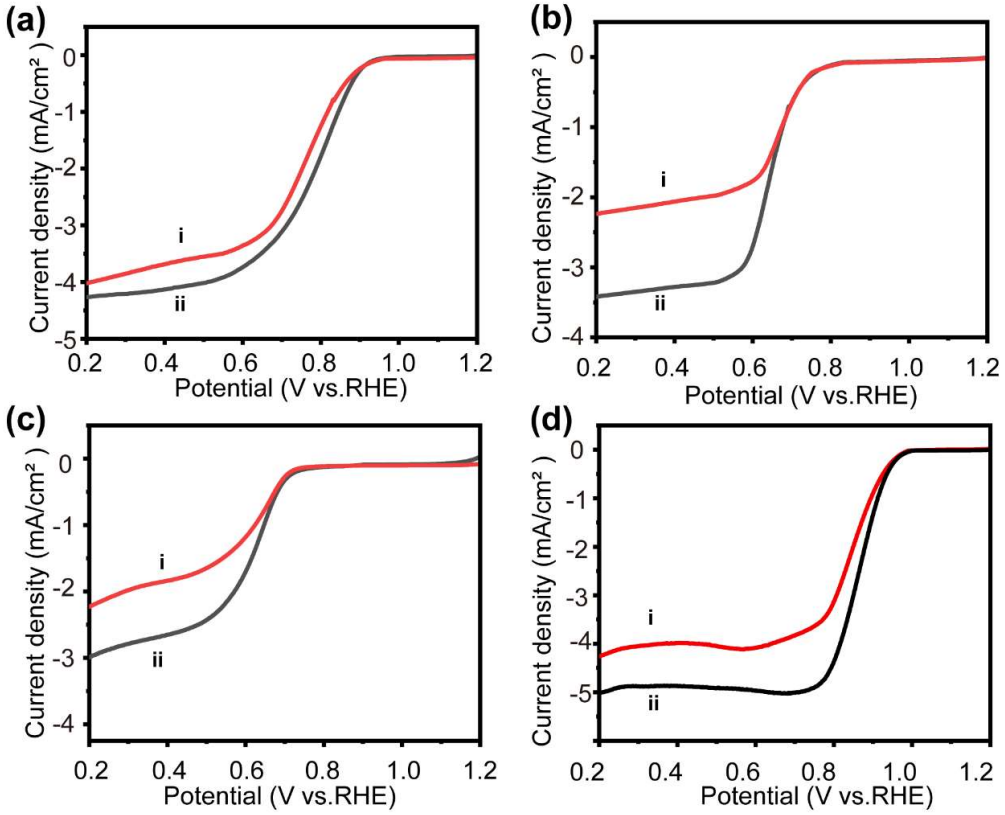

Fig. S12. LSV curves of (a) FeN@FCS-900, (b) N@FCS-900, (c) C_{60}-900, (d) Pt/C in O_2-saturated 0.1 M KOH solution at 1600 rpm; (i) before and (ii) after 5000 potential cycles.

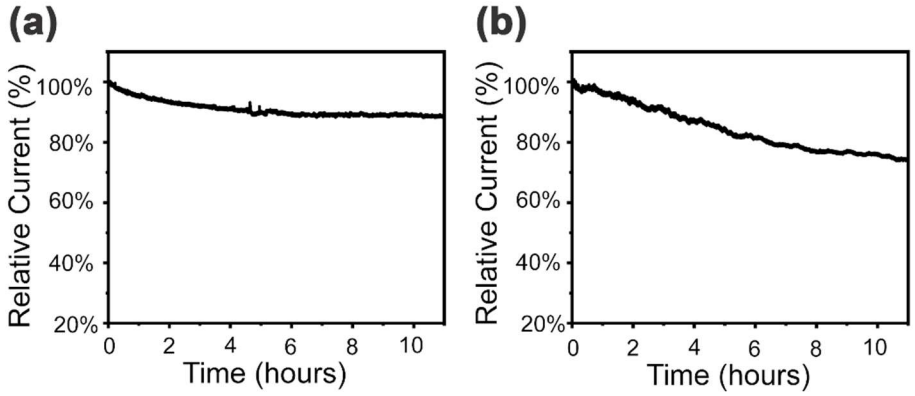

Fig. S13. Chronoamperometric response plots of (a) FeN@FCS-900 and (b) Pt/C in O_2-saturated 0.1M KOH solution.

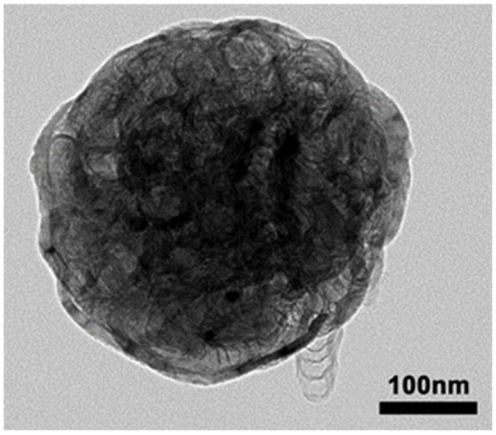

Fig. S14. TEM image of FeN@FCS-900 after the ORR process.

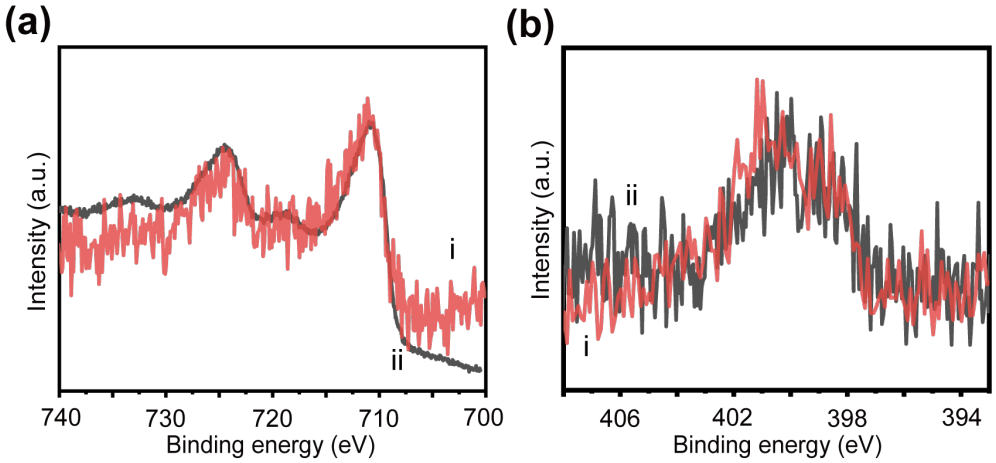

Fig. S15. (a) Fe 2p spectra and (b) N 1s spectra of FeN@FCS-900 (i) before and (ii) after the ORR process.

Table S1. The comparison of the ORR performance with various reported metal-doped carbon materials.

Sample name	E_{onset} (V)	$E_{1/2}$ (V)	j_L (mA)	*Ref.*
FeN@FCS-900	0.93	0.78	4.2	This work
L-FeNC	0.97	0.89	5.2	R1
M15-FeNC-NH_3	0.88	0.78	6.14	R2
SC-Fe	0.96	0.87	5.7	R3
Co@NCNTs	1.01	0.87	5.8	R4
Cu(15%)-MFC_{60}	0.86	0.76	5.18	R5
FMN700	0.93	0.81	4.7	R6
Fe-MFC_{60}	0.85	0.78	3	R7
N,S-PCNFs	0.96	0.83	5.50	R8
MFC_{60}-130	0.82	0.76	2.7	R9
MFC_{70}-150	0.86	0.75	5.5	R10
PD- C_{60}	0.89	0.78	4.8	R11

Reference in Table S1.

R1. X. Jiang, J. Chen, F. Lyu, C. Cheng, Q. Zhong, X. Wang, A. Mahsud, L. Zhang and Q. Zhang, *J. Energy Chem.*, 2021, **59**, 482-491.

R2. X. Xu, X. Zhang, Z. Xia, R. Sun, H. Li, J. Wang, S. Yu, S. Wang and G. Sun, *J. Energy Chem.*, 2021, **54**, 579-586.

R3. J. Xie, B. Q. Li, H. J. Peng, Y. W. Song, J. X. Li, Z. W. Zhang and Q. Zhang, *Angew. Chem., Int. Ed.*, 2019, **131**, 5017-5021.

R4. S. Chao, P. Liu, Q. Xia, S. Liu, W. Chen, W. Li and T. Ni, *CrystEngComm*, 2021, **23**, 1671-1676.

R5. G. Saianand, A. I. Gopalan, J. C. Lee, C. Sathish, K. Gopalakrishnan, G. E. Unni, D. Shanbhag, V. D. Dasireddy, J. Yi and S. Xi, *Small*, 2020, **16**, 1903937.

R6. Z. Peng, Q. Jiang, P. Peng and F.-F. Li, *Eng. Sci.*, 2021, **14**, 27-38.

R7. M. R. Benzigar, S. Joseph, G. Saianand, A.-I. Gopalan, S. Sarkar, S. Srinivasan, D.-H. Park, S. Kim, S. N. Talapaneni and K. Ramadass, *Microporous Mesoporous Mater.*, 2019, **285**, 21-31.

R8. Z. He, P. Wei, N. Chen, J. Han and X. Lu, *Chem.-Eur. J.*, 2021, **27**, 1423-1429.

R9. M. R. Benzigar, S. Joseph, H. Ilbeygi, D. H. Park, S. Sarkar, G. Chandra, S. Umapathy, S. Srinivasan, S. N. Talapaneni and A. Vinu, *Angew. Chem., Int. Ed.*, 2018, **57**, 569-573.

R10. M. R. Benzigar, S. Joseph, A. V. Baskar, D. H. Park, G. Chandra, S. Umapathy, S. N. Talapaneni and A. Vinu, *Adv. Funct. Mater.*, 2018, **28**, 1803701.

R11. J. Zhu, Y. Huang, W. Mei, C. Zhao, C. Zhang, J. Zhang, I. S. Amiinu and S. Mu, *Angew. Chem., Int. Ed.*, 2019, **58**, 3859-3864.